Rapid Crewed Missions to Mars: Impulsive Case

Filipe Alexandre da Costa Guerreiro Teixeira
filipe.a.c.g.teixeira@tecnico.ulisboa.pt

Instituto Superior Técnico, Univeridade de Lisboa, Portugal

January 2021

Abstract

Traditional minimum-energy transfers have a long transfer time (one leg) of about 259 d. Additionally, a stay of about 453 d is required to wait for the optimal return conditions. Such long times increase the risks posed by radiation and reduced gravity environments. These can be reduced by going faster, but lead to mass penalties. Since mass and time are proxies for cost and risk, respectively, rapid trips have lower risks but higher costs. In order to assess the impact of several choices in the overall mass, required elements for each mission architecture were identified and its mass estimated. Representative propulsion systems were selected, for actual and for future systems. For propellant mass estimations, the rocket equation was modified in order to include gravity losses and the disposal of empty tanks during manoeuvres. The former lead to new effects, unperceived by the traditional equation, such as the existence of a minimum total trip time. Obtained results suggest that rapid missions may not yet be achievable with reasonable mass. However, they are encouraging for the near future. As a comparison, the Design Reference Architecture 5.0, the benchmark in crewed Mars exploration, states an Initial Mass in Low Earth Orbit of 849 t for a total trip time of 916 d. For the same mass, a duration of 200 d can be achieved with a specific impulse of 1 000 s and a thrust-to-weight ratio of 75.
Keywords: crewed space missions, Mars, rapid transfers, space mission design

1. Introduction

1.1. Challenges of Crewed Missions to Mars

When considering interplanetary travels to Mars, minimum-energy transfers tend to be chosen. Although this is a measure to reduce the mission mass, the travel time is largely compromised. For one-way missions, the outbound travel takes around 259 d [1]. For round trips (e.g. sample returns and most crewed missions), a stay of about 453 d is also required to wait for the return conditions [1].

Such extensive times imply a long exposure to dangers such as radiation and reduced gravity, both present during the travel and the stay. Galactic cosmic radiaton is the long-term predominant form of radiation [2], while solar particle events are sporadic and well correlated with the Sun's period of most intense activity [2]. As for reduced gravity, significant, long-term physiological changes are induced: blood loss, muscle atrophies, bone demineralisation, fatigue and performance loss [3].

Rapid missions mitigate these adversities by decreasing the exposure time. However, much higher changes in velocity are required in order to achieve significant reductions [4]. Since mission mass and duration can be defined as a proxy to cost and risk, respectively, minimum-energy transfers minimise the mission cost by accepting higher risks while rapid missions minimise the risk by accepting higher costs.

1.2. Literature Review

Several proposals have been made in an effort to assess costs and risks of different options for crewed missions to Mars. Of particular importance is the Design Reference Architecture (DRA) 5.0 [5], which constitutes a benchmark for the community. Nonetheless, the relevance of some architectural choices are questionable [6]. Of these, crew size is perhaps the most important due to its large impact across most systems [6, 7].

Some proposals to lower the required velocity changes include Venus flybys [8], cycler orbits [9] and a rotating tether system [10]. However, none of these enable rapid missions in the range considered in this work.

Rapid crewed missions to Mars have already been addressed and were found competitive with the DRA 5.0 [1, 4]. However, the focus was primarily on the design of the interplanetary portion, and did not delve as deep in the system engineering aspects. Another study focused on the comparison of four propulsion systems (including future proposals) and reported difficulties in obtaining significant reductions for the total travel time [11]. Still,

that conclusion was drawn in the absence of In Situ Resource Utilisation (ISRU) and aerocapture, and the parameters for the selected propulsion systems might have been overly conservative.

2. Mission Design

2.1. Architectural Choices

There are myriad ways of reaching Mars. Distinct features, such as ISRU or a different crew size, require different plans, each with its own corresponding mass. In order to analyse and compare these options, the required elements must be identified, pieced together into a coherent architecture and its mass estimated. Only then can the overall mass of each architecture be estimated and weighted against its benefits.

At each stage, there are multiple choices:

- Crew size [5, 7, 12, 13]: between one and six.
- Cargo pre-deployment [5, 14]: yes or no.
- Mars Orbit Insertion (MOI) [5, 6, 15]: direct, all-propulsive or aerocapture.
- Entry, Descent and Landing (EDL) strategy [6]: all-propulsive, rigid aeroshell or Inflatable Atmospheric Decelerator (IAD).
- ISRU [5, 6, 16, 17]: none, atmosphere-based or atmosphere-based with regolith.
- Surface power system [5]: Solar Power System (SPS) or Fission Surface Power System (FSPS).
- Return strategy [18, 19]: skip-entry or all-propulsive.
- Propulsion [11]: impulsive thrust or continuous thrust.

From here, individual trades were conducted. Initial Mass in Low Earth Orbit (IMLEO) was chosen as the figure of merit due to its widespread use and consensus in being a well defined cost metric [20]. The focus of this work is then to assess the impact of options where there is no clear choice. When such options required an entirely in-depth analysis, a conservative approach was taken and possible issues identified.

Independently of the architecture, all missions must include a Transit Habitat (THAB) and the associated propulsion system, propellant and propellant tanks. The last are predicted to be numerous for rapid missions, and are discarded during the manoeuvres when empty. This is the bare minimum for an Apollo-like mission to Mars, with reduced exploration goals when compared to long-stay missions. Nonetheless, other elements may or may not be included depending on the specific architecture. In line with the DRA 5.0, the following elements were also incorporated: Mars Descent Module (MDM), Surface Habitat (SHAB), surface power system, Mars Ascent Vehicle (MAV) and re-entry capsule [5].

Generally, the mission can be divided into a crewed mission and two cargo missions. Cargo mission I carries elements that can be left in orbit, while cargo mission II delivers onto the surface the elements required for the stay. Surface deployment is done with the aid of MDMs.

In every case, the crew departs in the THAB, which is put into a high-energy Mars parking orbit upon arrival. Return propellant tanks are then loaded from the cargo spacecraft into the THAB. Next, the crew descends to the surface, performs the required activities and ascends in the MAV when the stay is over. The MAV then carries the astronauts back to the THAB for the return journey. When approaching Earth, the crew shifts into the re-entry capsule and the THAB is discarded. Propulsive manoeuvres are used throughout except in this last stage, where it may not be needed (discussed further in Section 2.2.8).

Specifically, operations differ only in the descent and ascent portion of the mission. For architectures including ISRU, the MAV needs to be sent onto the surface in order to be fuelled. In this case, the SHAB is used by the crew for the descent. This is not required for architectures without ISRU, in which the SHAB can be sent to the surface and the MAV used for both descent and ascent.

A crew of two is the obvious choice to minimise mass [13]. Crew size has a big impact in numerous subsystems, be it direct (e.g. life support system) or indirect (e.g. EDL and aerocapture) [7]. Typical values range from three to six astronauts, selected in a top-down manner [5, 7, 12, 21], but can be as low as one [13]. It has been suggested that any crew should feature at least one member per each type of personnel: an engineer or technician, a geologist or biologist, and a doctor [7]. However, functions performed by a doctor can be bypassed for shorter missions. Unlike longer ones, the reduction in exposure to the risk environment decreases the value that a doctor might have.

Cargo was chosen to be pre-deployed in separate spacecrafts. Sending the crew in a fast trajectory is a measure to reduce exposure to space hazards. This comes at the expense of a large mass penalty but the same requirement does not apply to the cargo, which can be sent in a low energy transfer at a prior date. Doing so leads to longer systems cumulative time but significantly reduces the total IMLEO [5].

Propulsive braking was selected as the method

for MOI. Direct entry is not adequate for the fast mission concept. The associated velocities are large and Mars' atmosphere is thinner than Earth's. Aerocapture is usually an option to lower propellant mass, but it was not considered in this work because it poses serious challenges in this context. Namely, can the propulsion system stay attached during the manoeuvre, or is another system required for the return trip? Can solar panels be retracted during the manoeuvre? Can the Thermal Protection System (TPS) be re-utilised? Can aerocapture support the typically large payloads associated with crewed missions? Furthermore, aerocapture loses some of its value when applied to fast missions. For such large velocities, most of the braking would likely have to be done with propellant anyway. Aerocapture has huge difficulties that must be addressed in an in-depth study that lies outside the scope of this work.

For the EDL, a rigid aeroshell was chosen. All-propulsive solutions were not selected due to the large payload mass fractions expected [5]. As for IADs, initial DRA 5.0 data was lacking in the desired range and extrapolations were too big to be considered acceptable [5]. A detailed EDL analysis was not performed, and the required values were taken from DRA 5.0 instead.

ISRU for Mars ascent propellant production was left open for comparison. If an atmosphere-based approach is selected, methane has to be carried from Earth. On the other hand, all the required elements can be produced on-site if water is retrieved from Martian regolith [17]. However, additional equipment is necessary in order to mine it. Besides, the operation of said equipment, like excavators and haulers, has unresolved significant challenges [5].

The surface power system decision is dependent on the ISRU strategy. For architectures employing ISRU, a FSPS was chosen [5]. This allows a continuous operation of the ISRU plant while a SPS is limited to eight hours per day and results in higher power needs [5]. Additionally, the former has a lower mass and it is easier to deploy autonomously [5]. Without ISRU both options are left open. The crew can deploy the solar arrays on arrival, eliminating the complexities associated with autonomous deployment. Lower power requirements [5] also reduce system mass making the solar option more competitive.

The preferred return strategy is the skip entry, which naturally encompasses direct entries (i.e. skip entries with zero skips). Direct entries are more easily controlled, but skipping in the atmosphere allows for cool-down periods which limit the amount of aerodynamic heating [19]. Historically, difficulties stemmed from computational limitations [19], but improvements in Earth approach navigation [22] have reduced this issue. A skip entry is also endorsed in the DRA 5.0 [18]. Nonetheless, some cases require some degree of propulsive braking in order to cope with the re-entry limits (further details in Section 2.2.8).

Summarising, the considered options regarding the ISRU and the surface power system are listed in Table 1.

ISRU	Surface power system	Option
None	SPS	A
None	FSPS	B
Atmosphere-based	FSPS	C
Atmosphere-based with regolith	FSPS	D

Table 1: Considered ISRU and surface power system options.

2.2. Mass Budget

2.2.1 Consumables

In order to estimate the mass of the consumables, a choice must be made between an open- and a closed-loop Environmental Control and Life Support System (ECLSS). For this end, data from available International Space Station (ISS) recycling systems [23] was adapted to this context. Since they would not be used long enough to compensate their mass, the open-loop ECLSS was selected.

Consumables are required on a per day per crewmember basis. Water requirements encompass hydration, food rehydration and personal hygiene, for a total of 2.9 kg [24]. Other consumables are comprised of food (2.39 kg, including packaging [25]), oxygen (0.82 kg [25]) and lithium hydroxide (1.75 kg [23]) for carbon dioxide removal. Each kilogram of oxygen, and water, also require 0.236 kg and 6.136×10^{-3} kg, respectively, worth of storage tanks [26]. The remaining consumables amount to 182.5 kg (one time), 51.625 kg (one time per crewmember), 0.312 5 kg (per day) and 1.813 3 kg (per day per crewmember) [26].

2.2.2 Mars Transit and Surface Habitats

At a high level, the THAB can be divided into structure, radiation shielding, accommodations and subsystems. Data and methedology was adapted from several sources [5, 26, 27], and resulted in Table 2. The SHAB is designed for a smaller duration, but shares the same characteristics of the THAB. Since it does not need to produce its own energy, the SHAB mass budget is the same except for the subsystems mass, which is 2 977.4 kg.

Element	Mass, kg
Structure	$122.6\left(N_{\text{crew}}d^{0.6}\right)^{2/3}$
Radiation shielding	$804.4\left(N_{\text{crew}}d^{0.6}\right)^{2/3}$
Accommodations	670.9
Subsystems	4 010.0

Table 2: THAB mass budget.

2.2.3 Crew and Samples

When estimating crew mass, an average of 82 kg was used for each crewmember [25].

For samples, the total mass was assumed to be 239 kg [28]. 10 containers, each with a mass of 1.1 kg, were also selected to transport the samples [28].

2.2.4 Mars Descent Module

The MDM is in charge of landing payloads to the surface of Mars. This includes the ISRU plant, the SHAB and the MAV. The main components were adapted from the DRA 5.0 Addendum II [29], and totalled 28 728.3 kg.

2.2.5 Mars Ascent Vehicle

The MAV ferries the crew from Mars surface back into the parking orbit, where it meets the THAB for the return trip. Choosing a more energetic orbit means that the THAB does not have to brake or accelerate as much when reaching or leaving Mars, respectively. However, it is also harder for the MAV to reach said orbit. The best compromise in order to alleviate the propellant needs of the THAB was a 250 km × 119 450 km orbit with a corresponding period of 5 sol [28]. Data was adapted from [28], and resulted in a liftoff mass of 46 769 kg, from which 27 968 kg and 8 892 kg is liquid oxygen and liquid methane, respectively.

2.2.6 In Situ Resource Utilisation

Based on the requirements of Section 2.2.5, four units in parallel are needed to produce the ascent propellant, independently of the selected ISRU type. A continuous production during 480 day (with typical regolith when applicable) were assumed [17]. These units have a combined mass and power consumption of 1 200 kg and 45.3 kW, respectively, for atmosphere-based ISRU. If regolith is also mined, the values increase to 2 267 kg and 69.3 kW, respectively.

2.2.7 Surface Power System

Depending on the architecture chosen, there are two types of surface power system: solar or nuclear. For scenarios without ISRU (options A and B), the SHAB is the only power concern. Otherwise (options C and D), there are two phases: ascent propellant production, during which only the ISRU plant is being used, and crewed phase, where all propellant has already been produced and only the SHAB needs to be powered. ISRU power needs surpass by far the ones from the SHAB, thus being the driver.

The mass of the surface power system resulted in 5 838 kg, 5 423 kg, 10 450 kg and 13 450 kg for options A, B, C and D, respectively. The values were obtained by extrapolating the data present in DRA 5.0 and include an extra 20 % contingency [5].

2.2.8 Re-Entry Capsule

Re-entry is typically limited by the amount of heat the spacecraft can dissipate, along with g-force limits for crewed missions. Since the interplanetary travel velocities are large for rapid missions, particular care needs to be taken when sizing the re-entry capsule.

The TPS mass fraction correlates well with the total heat load, and a fit based on historical data for ablative shielding is given by [30]

$$\chi = 9.1 \times 10^{-4} \left(Q \times 10^{-4}\right)^{0.515\,75}, \qquad (1)$$

where χ is the TPS mass fraction and Q is the total heat load in $\mathrm{J\,m^{-2}}$. Determining the exact heat load is not easy, and often requires a detailed simulation of the re-entry environment. Here, a conservative estimate was done, which is meant to be refined by further work. The use of lift can open new re-entry trajectories [22], but is another convoluted topic. For the sake of simplicity, it was assumed that no lift was acting on the capsule and the ballistic re-entry equations of motion [27, 31] were numerically solved for the 1976 US Standard Atmosphere [27]. Then, both conductive [27] and radiative [32] heating rates were integrated to provide the total heat load. Apollo data [27, 30] was used as a benchmark since it is readily available and flight proven.

The afore analysis was repeated for several velocities at Earth infinity. For each, the arrival hyperbolic orbit impact parameter was varied as to provide the lowest TPS mass fraction possible. The resulting data can be seen in Table 3, and an interpolation was used when needed. For a velocity of $11\,\mathrm{km\,s^{-1}}$, no solution was found. Therefore, for velocities larger than $10\,\mathrm{km\,s^{-1}}$, a propulsive braking was used to reduce it to this value. Doing so at the perigee (inside Earth's atmosphere) may be difficult or even infeasible. On the other hand, braking at

Earth infinity is inefficient but allows for plenty of time to execute the manoeuvre and perform security checks. It was opted to brake at Earth infinity for both simplicity and to be conservative, but this topic should be investigated further.

Velocity at Earth infinity, $\mathrm{km\,s^{-1}}$	TPS mass fraction, %
7	31.2
8	37.7
9	46.5
10	58.5

Table 3: Velocity at Earth infinity and corresponding TPS mass fraction.

2.2.9 Propellant

For propellant estimations, consider the rocket equation, given in non-dimensional form by [33]

$$\Delta v = -gI_{\mathrm{SP}} \log\left[\epsilon + (1-\epsilon)\varpi\right], \tag{2}$$

where Δv is the total change in velocity, g is the gravitational acceleration at Earth's surface ($9.806\,7\,\mathrm{m\,s^{-2}}$ [27]), I_{SP} is the specific impulse of the engine, $\epsilon = m_s/(m_s + m_p)$ is the structural ratio, m_s is the structural mass, m_p is the propellant mass, $\varpi = m_*/m_0$ is the payload ratio, m_* is the payload mass and m_0 is the mass at the start of the manoeuvre.

Finite burn losses can be incorporated as

$$\Delta v = \Delta v_{\mathrm{ideal}} + \Delta v_{\mathrm{losses}}, \tag{3}$$

where $\Delta v_{\mathrm{ideal}}$ is the ideal change in velocity (from an impulsive manoeuvre) and $\Delta v_{\mathrm{losses}}$ is the extra amount needed to compensate the losses. An estimate of the latter is given by [34, 35]

$$\Delta v_{\mathrm{losses}} = \frac{1}{24}\frac{\mu}{r^3} {t_{\mathrm{burn}}}^2 \Delta v_{\mathrm{ideal}}, \tag{4}$$

where μ is the gravitational parameter of the primary, r is the distance to the primary when executing the impulsive manoeuvre and t_{burn} is the time for the propellant to be burnt. This is a conservative estimate, since actual burn losses can be smaller by up to a factor of two [35]. The burn time is a function of the propellant mass through [35]

$$t_{\mathrm{burn}} = \frac{gI_{\mathrm{SP}}}{T} m_p, \tag{5}$$

where T is the thrust. Using Eqs. (2) to (5), the modified rocket equation can be written as

$$\begin{aligned} &\Delta v_{\mathrm{ideal}} \left[1 + \frac{1}{24}\frac{\mu}{r^3}\left(\frac{gI_{\mathrm{SP}}}{T}\right)^2 {m_p}^2\right] = \\ &= -gI_{\mathrm{SP}} \log\left[\epsilon + (1-\epsilon)\varpi\right]. \end{aligned} \tag{6}$$

In order to include the gains from the disposal of empty propellant tanks, an analogy was made with a rocket with N stages [33]. The structural ratio and payload ratio can be defined for each stage [33], and assuming that the same tank technology is used, the structural ratio is also the same [33]. This result is independent of the relation between tank mass and propellant mass.

But in order to calculate the structural factor, it was also assumed that the tank mass was proportional to the propellant mass. In principle, it should be proportional to the two-thirds power of the latter, since it scales with the tank surface area instead of the tank volume. However, the deposits arrangement and connections should also be more complex as the number of tanks increases, leading to higher masses. In order to take a conservative approach, the linear relation was kept. Data retrieved for common chemical propellants[1] and propellant tanks[2] resulted in a stage structural ratio ϵ_k of about 0.038.

Assuming that the propellant tanks all have the same size,

$$m_{p_k} = m_p/N, \tag{7}$$

where m_{p_k} is the propellant mass of the k-th stage. Since the payload of the k-th stage is the initial mass of stage $k+1$, it is possible to find recurrence relations by accounting the initial mass, propellant mass, structural mass and payload mass of the k-th stage. These can be re-written in terms of the stage structural and payload ratios, and it can then be shown that the closed-form solution for former is given by

$$\varpi_k = \frac{m_*(1-\epsilon_k) + (N-k)m_p/N}{m_*(1-\epsilon_k) + (N-k+1)m_p/N}, \tag{8}$$

when the tanks are equal, i.e. same technology and size. Since Eq. (6) is applicable to each stage, the overall change in velocity is the sum of the contributions of each stage. In the context of rapid missions, propellant mass is expected to be considerable. Thus, a high number of propellant tanks of regular size can be used, and the limit when N tends to infinity taken. Overall, this leads to

$$\begin{aligned} m_p = m_*(1-\epsilon)\Bigg(&\exp\left[\frac{1}{1-\epsilon}\frac{\Delta v_{\mathrm{ideal}}}{gI_{\mathrm{SP}}}\cdot\right. \\ &\left.\cdot\left(1 + \frac{1}{24}\frac{\mu}{r^3}\frac{g^2 {I_{\mathrm{SP}}}^2}{T^2} {m_p}^2\right)\right] - 1\Bigg). \end{aligned} \tag{9}$$

[1] Braeunig, R. A.,"Rocket Propellants," `http://www.braeunig.us/space/propel.htm`, 2008. Retrieved 17 December 2020.

[2] Astrium, "Propellant Tanks for Spacecraft," `https://www.yumpu.com/en/document/view/17516891/propellant-tanks-for-spacecraft-astrium-st-service-portal-eads`, 2013. Retrieved 15 December 2020.

This is similar to the traditional rocket equation but accounts for both the tank mass (assuming each tank is disposed when empty and small enough for the continuous approximation to be valid) and finite burn losses. Thus, Eq. (9) was used throughout the work for the propellant estimations.

3. Propulsion

3.1. Overview

In this work only impulsive manoeuvres were considered, which corresponds to a high-thrust scenario. The case of continuous thrust manoeuvres will be analysed in a future work.

Propulsion systems are characterised by two parameters: specific impulse and thrust-to-weight ratio. The first is a measure of its efficiency, while the latter expresses its acceleration in multiples of Earth's gravitational acceleration. Thrust itself is not characteristic of the system since engines can be, to a certain degree, added in parallel. Figure 1 shows these two parameters for several modern and proposed propulsion systems [36]. Chemical systems are characterised by a high thrust-to-weight ratio but relatively low specific impulse. These are at least at a Technology Readiness Level (TRL) of six. Non-chemical systems (for instance electrical), are more efficient but tend to produce smaller accelerations. Although some are at a TRL of nine, others can be as low as three. Lastly, advanced systems values do not follow a specific trend. Available information is estimated since the TRL is, at most, three.

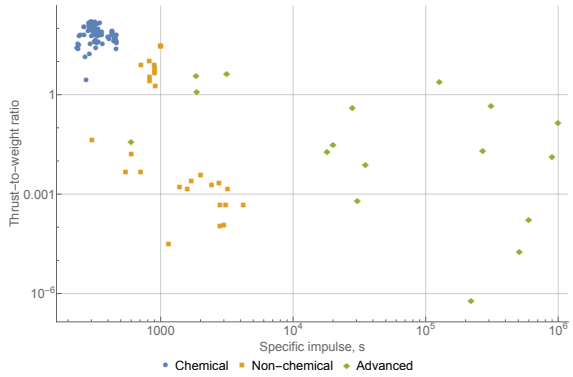

Figure 1: Specific impulse and thrust-to-weight ratio for several modern and proposed propulsion systems. Data retrieved from [36].

3.2. Representative Values for High Thrust Propulsion Systems

In order to select representative values for the propulsion system parameters, points with highest thrust-to-weight ratios for a given specific impulse (corresponding to the high thrust scenario) were identified in Fig. 1. A linear regression (in logarithmic scale) was then made, and optimistic and pessimistic curves were drawn. These were shifted by symmetric amounts regarding the regression. Finally, points were chosen at regular specific impulse intervals, with the corresponding thrust-to-weight ratios being rounded for ease in display. This resulted in

$$T/W = c{I_{\mathrm{SP}}}^{-0.8}, \tag{10}$$

where T/W is the thrust-to-weight ratio, I_{SP} is the specific impulse in s and c is 8 826.2, 15 887.1 and 4 903.4 for the regression, optimistic curve and pessimistic curve, respectively.

3.3. Cases Studied and Assumptions

The considered cases are summarised in Table 4, for which the values were taken from the optimistic curve. Due to time constraints, pessimistic values were not analysed but are scheduled to be addressed in a future work. For a first impression, the optimistic values were deemed more useful since this work took a conservative approach on most topics that required further study. If values from the pessimistic curve were taken instead, the results could have been too overestimated.

Case	Specific impulse, s	Thrust-to-weight ratio
I	3×10^2	190.0
II	1×10^3	75.0
III	3×10^3	32.0
IV	1×10^4	12.6
V	3×10^4	5.4

Table 4: Studied values for the propulsion system parameters.

Propulsion systems with lower thrust-to-weight ratios will also be studied in future works. These are not adequate for an impulsive approach, but may be useful in a continuous thrust scenario. This requires a different approach than the Lambert's solver employed in this work, and should be studied separately.

Systems categorised as advanced in Fig. 1 have notoriously low TRL values, implying that the values are speculative and uncertain. It may seem unrealistic to include them in such analysis, but there is merit in doing so. With the propulsion of today, rapid trips to Mars require large amounts of propellants that lead to exceedingly high values for IMLEO. Will this paradigm change? Does any of the currently proposed systems, even if somewhat farfetched, enable rapid travels with reasonable mass? These are the type of questions that can be answered by encompassing these systems.

Lastly, two important assumptions were made. First, it was considered that engines could be added

in parallel in order to ensure the high thrust required for the impulsive scenario. This essentially turns the thrust (or equivalently the number of engines) into a design parameter, which can be varied to yield the best result. Second, some propulsion systems also require a separate power source. When applicable, and unless otherwise stated by the source, it was considered that this was included in the thrust-to-weight ratio of the system.

4. Results

The trade-off between IMLEO and total trip time (proxies for cost and risk, respectively) is considered for several architectures. Each includes a distinct combination of the options referred in Table 1 with the propulsive systems selected in Table 4, for a total of 20. Only rapid trips with short stays were studied, in order to avoid the long waiting times associated with longer, more economic missions. This way, the exposure to radiation and microgravity environments is minimised.

Due to time constraints, only a stay of 30 d was considered (consistent with the duration mentioned in the DRA 5.0 for short-stay missions [5]) but more will be analysed in a future work. All times were counted from an opposition configuration. Time resolution was variable, depending on the needs, but was no higher than 1 d.

In the following results, the total trip time includes the stay time (since it is also an exposure to a risk environment [37, 38]). IMLEO was also capped at 10^5 t. Although this might seem excessive for today's standards, it is meant to give a perspective of what might be achievable in the future. Typically, IMLEO can go up to around 1 000 t [4, 5] but there is an effort to reduce launch costs by a factor of 100[3]. Thus, an IMLEO of 100×10^3 t $= 10^5$ t might become reasonable.

4.1. Influence of the Specific Impulse and Thrust-to-Weight Ratio

All of the studied cases display the same general behaviour, despite ocurring significant changes to minimum travel time, IMLEO range and IMLEO for longer missions, depending on the selected propulsion system. The Pareto front for each propulsion case (recall Table 4) is shown in Fig. 2 for option A (recall Table 1). Options B, C and D yielded very similar results.

For the propulsion case I, only a section of the curve appears since even for the largest times considered, the IMLEO ranges from about 3×10^4 t to 10^5 t.

[3]Galeon, D., "Elon Musk: With New SpaceX Tech, Rocket Costs Will Drop by a Factor of 100," https://futurism.com/elon-musk-with-new-spacex-tech-rocket-costs-will-drop-by-a-factor-of-100, September 2017. Retrieved 30 December 2020.

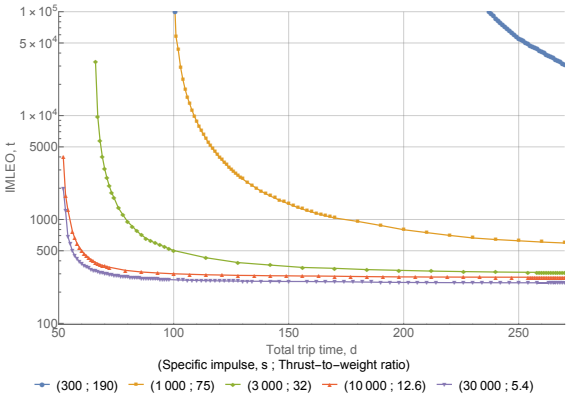

Figure 2: Pareto fronts for option A and propulsion cases I through V, with a stay time of 30 d.

When progressing from propulsion cases I through V, the best IMLEO for a certain time starts decreasing. This variation is large at first, but it gets progressively smaller. For 250 d, for instance, compare the massive reduction from about 6×10^4 t to about 700 t (from case I to case II) with the less significant reduction from the latter to about 300 t (from case II to case III). From case III onwards, the gains in IMLEO are even smaller. Furthermore, the gains are larger for faster trips.

The gains in minimum total trip time exhibit a similar behaviour to those in the IMLEO. For propulsion case I, the minimum total trip time is not present in the plots since it leads to masses higher than 10^5 t. From cases II to IV, it is about 100 d, 65 d and 50 d, respectively. Case V shares the same minimum total trip time of case IV.

From the above results, it can be concluded that propulsion case I does not fit the rapid mission archetype. Since this case is mostly representative of today's propulsion technology limits, rapid missions are likely not yet achievable with a reasonable IMLEO.

Furthermore, it can be inferred that when progressing from propulsion cases I through V, the beneficial effects (i.e. increasing the specific impulse) dominate at first. However, these eventually become comparable with the adverse effects (i.e. decreasing the thrust-to-weight ratio).

4.2. Comparison Between Architectures

In order to compare the studied architectures, the results were plotted together in Fig. 3. The figure is a little confusing, but that itself is the key point to be taken. Differences in the studied options (Table 1) have minor influences, which only become noticeable when the curves start to flatten. This happens because, for faster missions, a higher portion of the IMLEO is constituted by propellant mass. When the curves start to flatten, corresponding to

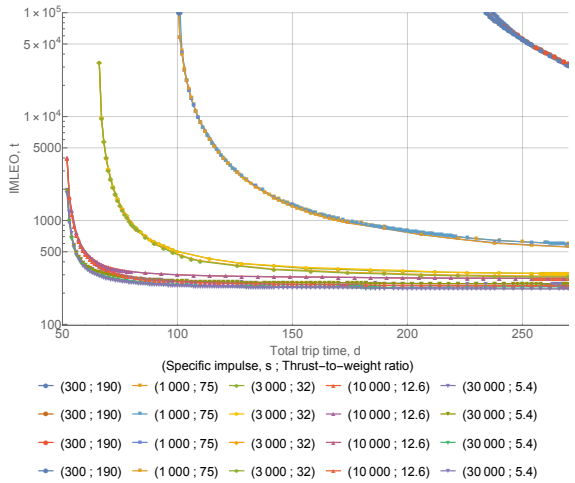

Figure 3: Pareto fronts for options A through D and propulsion cases I through V, with a stay time of 30 d. The first, second, third and fourth row in the legend correspond to options A, B, C and D, respectively.

lower propellant masses, the differences between the options become more noticeable. Thus, the analysed options are more relevant for minimum energy transfers, where the mass is more evenly distributed between elements, than for rapid round trips, where most of the mass stems from the propellant. The effect may appear more prominent for higher specific impulses, but that stems from the logarithmic scale used in the plots. Overall, architectures are mostly dependent on the characteristics of the propulsion system.

It is important to recall that ISRU is only being considered for the production of ascent propellant. In fact, were it possible to produce the return fuel on Mars, IMLEO could be significantly lower. This should be addressed in a future work as it requires major changes in the architecture.

4.3. Relation Between Outbound and Return Travel Times

Besides the IMLEO, the relation between outbound and return travel times was also analysed. This was approximately linear with slightly faster outbound travels. Since all the propellant for the return trip must first be carried to Mars, it is less expensive to accelerate the outbound trip rather than the return one. Unsurprisingly, this holds for every propulsion case and every option since it is only related to the geometry of the interplanetary trajectories.

4.4. Implications for Rapid Missions to Mars

The unfavourable results for the propulsion case I, representative of today, indicate that rapid missions may not yet be achievable with a reasonable mass. However, the results are encouraging for the near future. In particular, the DRA 5.0 states an IMLEO of 849 t for a total trip time of 916 d. Even if one does not account for the large stay of 496 d [5], it still features a trip of 420 d. For the propulsion case II, the one most likely to be available in the near future, a mission with similar mass can be undertaken in about 200 d, corresponding to a trip of about 170 d. This corresponds approximately to a 59.5 % decrease in travel time (excluding stay), or a 78.2 % decrease in total trip time. The time can be decreased further, for propulsion cases III through V, but each case is farther away in the future. Overall, rapid crewed missions to Mars are likely to become competitive with the traditional minimal-energy approach.

5. Conclusions

This work determines the trade-off between IMLEO and round trip time for rapid crewed missions to Mars with high thrust. The most promising architectures were identified, and the required elements estimated. Finally, different characteristic values were selected for both modern and foreseen propulsion systems.

It has been found that there is a minimum value for the travel time, which depended on the characteristics of the propulsion system used. Such limit stemmed from the inclusion of a burn losses term in the rocket equation. Due to that same term, there is an optimum thrust value that yields the lowest IMLEO for a certain total trip time. This behaviour differs greatly from the traditional rocket equation, for which there is a solution to every total trip time. In the ideal case, the propellant mass increases monotonically with thrust through the propulsion system mass (with higher increases for lower thrust-to-weight ratios).

The large amount of propellant required constitutes most of the mass. For this reason, all considered architectures performed equally for faster missions and showed only small differences for slower ones. In particular, the usage of ISRU for the production of ascent propellant makes no significant difference for rapid trips.

Finally, this work suggests that this type of mission can be possible in the future. For comparison, DRA 5.0 states an IMLEO of about 849 t for a round trip time of 916 d [5]. For the same mass, the mission can be achieved in about 200 d with case II propulsion.

5.1. Future Work

This work is a first approach to address the problem, and was developed at the level of preliminary design. There are subjects in need of development, which require a dedicated approach. Some can be found in the literature, albeit in a non-applicable range for the rapid mission concept. Namely, burn

losses estimation, re-entry and aerocapture. Although the last should still be studied, chances are that the mass savings will not be significant enough (due to TPS limitations) in this same context, much like ISRU usage for Mars ascent propellant production. Trajectory-wise, the calculations need to be extended to the real case, with eccentric and non-coplanar orbits.

Of particular importance is whether or not ISRU can be used for the production of the return propellant. This will demand a considerable re-design of the mission in order to solve the problem of transporting the propellant to orbit. But with the vast majority of the IMLEO concentrated in the propellant, there is potential for large savings by producing it on site rather than carrying it from Earth.

Acknowledgements
The author would like to sincerely thank his family, for all the love and support provided through these years, as well as Professor Paulo Gil, for his guidance, patience and availability in mentoring this work.

References

[1] Wertz, J. R., "Interplanetary Round Trip Mission Design," *Acta Astronautica*, Vol. 55, No. 3, 2004, pp. 221 – 232. https://doi.org/10.1016/j.actaastro.2004.05.019.

[2] Tripathi, R. K., and Nealy, J. E., "Mars Radiation Risk Assessment and Shielding Design for Long-Term Exposure to Ionizing Space Radiation," *2008 IEEE Aerospace Conference*, 2008, pp. 1–9.

[3] Kanas, N., and Manzey, D., *Space Psychology and Psychiatry*, 2nd ed., Space Technology Library, Vol. 22, Springer, 2008. https://doi.org/10.1007/978-1-4020-6770-9.

[4] Amade, N. S., and Wertz, J., "Design of a Mars Rapid Round Trip Mission," *AIAA SPACE 2010 Conference & Exposition*, 2010. https://doi.org/10.2514/6.2010-8642.

[5] Drake, B. G. (ed.), *Human Exploration of Mars Design Reference Architecture 5.0*, NASA-SP-2009-566, 2009.

[6] Salotti, J. M., "New Trade Tree for Manned Mars Missions," *Acta Astronautica*, Vol. 104, No. 2, 2014, pp. 574 – 581. https://doi.org/https://doi.org/10.1016/j.actaastro.2014.07.017.

[7] Salotti, J. M., Heidmann, R., and Suhir, E., "Crew Size Impact on the Design, Risks and Cost of a Human Mission to Mars," *2014 IEEE Aerospace Conference*, 2014, pp. 1–9. https://doi.org/10.1109/AERO.2014.6836241.

[8] Hughes, K. M., Edelman, P. J., Longuski, J., Loucks, M., Carrico, J. P., and Tito, D. A., "Fast Mars Free-Returns via Venus Gravity Assist," *AIAA/AAS Astrodynamics Specialist Conference*, 2014. https://doi.org/10.2514/6.2014-4109.

[9] Landau, D., and Longuski, J., "A Reassessment of Trajectory Options for Human Missions to Mars," *AIAA/AAS Astrodynamics Specialist Conference and Exhibit*, 2004. https://doi.org/10.2514/6.2004-5095.

[10] Nordley, G. D., and Forward, R. L., "Mars-Earth Rapid Interplanetary Tether Transport System: I. Initial Feasibility Analysis," *Journal of Propulsion and Power*, Vol. 17, No. 3, 2001, pp. 499–507. https://doi.org/10.2514/2.5798.

[11] Guerra, A. G. C., Bertolami, O., and Gil, P. J. S., "Comparison of Four Space Propulsion Methods for Reducing Transfer Times of Manned Mars Mission," https://arxiv.org/abs/1502.06457, 2015.

[12] Zubrin, R., *The Case for Mars*, 1st ed., Simon & Schuster, 2011.

[13] Tito, D. A., Anderson, G., Carrico, J. P., Clark, J., Finger, B., Lantz, G. A., Loucks, M. E., MacCallum, T., Poynter, J., Squire, T. H., and Worden, S. P., "Feasibility Analysis for a Manned Mars Free-Return Mission in 2018," *2013 IEEE Aerospace Conference*, 2013, pp. 1–18. https://doi.org/10.1109/AERO.2013.6497413.

[14] Salotti, J. M., and Claverie, B., "Human Mission to Mars: All-up vs Pre-deploy." *Global Space Exploration Conference*, 2012.

[15] Spilker, T. R., Adler, M., Arora, N., Beauchamp, P. M., Cutts, J. A., Munk, M. M., Powell, R. W., Braun, R. D., and Wercinski, P. F., "Qualitative Assessment of Aerocapture and Applications to Future Missions," *Journal of Spacecraft and Rockets*, Vol. 56, No. 2, 2019, pp. 536–545. https://doi.org/10.2514/1.A34056.

[16] Starr, S. O., and Muscatello, A. C., "Mars In Situ Resource Utilization: A Review," *Planetary and Space Science*, Vol. 182, 2020, p. 104824. https://doi.org/https://doi.org/10.1016/j.pss.2019.104824.

[17] Kleinhenz, J. E., and Paz, A., "An ISRU Propellant Production System for a Fully Fueled Mars Ascent Vehicle," *10th Symposium*

on Space Resource Utilization, 2017. https://doi.org/10.2514/6.2017-0423.

[18] Drake, B. G. (ed.), *Human Exploration of Mars Design Reference Architecture 5.0 Addendum*, NASA/SP-2009-566-ADD, 2009.

[19] Young, J. W., and Smith, Jr., R. E., "Trajectory Optimization for an Apollo-Type Vehicle Under Entry Conditions Encountered During Lunar Return," Technical Report NASA-TR-R-258, NASA, May 1967.

[20] Ward, E. D., Webb, R. R., and deWeck, O. L., "A Method to Evaluate Utility for Architectural Comparisons for a Campaign to Explore the Surface of Mars," *Acta Astronautica*, Vol. 128, 2016, pp. 237 – 242. https://doi.org/https://doi.org/10.1016/j.actaastro.2016.07.022.

[21] Salotti, J. M., "Human Mission to Mars: The 2-4-2 Concept," Technical Report 2012-5-242, Institut Polytechnique de Bordeaux, May 2011.

[22] Putnam, Z. R., Braun, R. D., Rohrschneider, R. R., and Dec, J. A., "Entry System Options for Human Return from the Moon and Mars," *Journal of Spacecraft and Rockets*, Vol. 44, No. 1, 2007, pp. 194–202. https://doi.org/10.2514/1.20351.

[23] Jones, H. W., "Would Current International Space Station (ISS) Recycling Life Support Systems Save Mass on a Mars Transit?" *47th International Conference on Environmental Systems*, 2017.

[24] "Human Integration Desing Handbook," Special Publication NASA/SP-2010-3407/REV1, NASA, January 2014.

[25] Anderson, M. S., Ewert, M. K., and Keener, J. F., "Life Support Baseline Values and Assumptions Document," Technical Publication NASA/TP-2015-218570/REV1, NASA, January 2018.

[26] Boden, R. C., "Mass Estimation Tool for Human Space Missions," Master's thesis, Technische Universität München, 2013.

[27] Sforza, P. M., *Manned Spacecraft Design Principles*, Elsevier, 2016.

[28] Polsgrove, T. P., Percy, T. K., Rucker, M., and Thomas, H. D., "Update to Mars Ascent Vehicle Design for Human Exploration," *2019 IEEE Aerospace Conference*, 2019, pp. 1–15. https://doi.org/10.1109/AERO.2019.8741709.

[29] Drake, B. G., and Watts, K. D. (eds.), *Human Exploration of Mars Design Reference Architecture 5.0 Addendum #2*, NASA/SP-2009-566-ADD2, 2014.

[30] Laub, B., and Venkatapathy, E., "Thermal Protection System Technology and Facility Needs for Demanding Future Planetary Missions," *Planetary Probe Atmospheric Entry and Descent Trajectory Analysis and Science*, ESA Special Publication, Vol. 544, edited by A. Wilson, 2004, pp. 239–247.

[31] Chapman, D. R., "An Approximate Analytical Method for Studying Entry into Planetary Atmospheres," Technical Note NACA-TN-4276, NASA, May 1958.

[32] Tauber, M. E., and Sutton, K., "Stagnation-Point Radiative Heating Relations for Earth and Mars Entries," *Journal of Spacecraft and Rockets*, Vol. 28, No. 1, 1991, pp. 40–42. https://doi.org/10.2514/3.26206.

[33] Wiesel, W. E., *Spaceflight Dynamics*, 3rd ed., Aphelion Press, 2010.

[34] Robbins, H. M., "An Analytical Study of the Impulsive Approximation," *AIAA Journal*, Vol. 4, No. 8, 1966, pp. 1417–1423. https://doi.org/10.2514/3.3687.

[35] Confraria, J. C. F., "Finite Burn Losses in Spacecraft Maneuvres Revisited," Master's thesis, Instituto Superior Técnico, 2020.

[36] da Silva Rodrigues Pinto, J. T., "A Survey of Modern and Future Space Propulsion Methods," Master's thesis, Instituto Superior Técnico, 2019.

[37] Ding, Y., and Shen, Z., "Investigation of the Radiation Environment in Deep Space and Its Effect on Spacecraft Materials Properties," *Protection of Materials and Structures from the Space Environment*, edited by J. Kleiman, Springer International Publishing, Cham, 2017, pp. 471–479.

[38] Walberg, G., "How shall we go to Mars? A review of mission scenarios," *Journal of Spacecraft and Rockets*, Vol. 30, No. 2, 1993, pp. 129–139. https://doi.org/10.2514/3.11521.